Cell Traction Forces on Soft Biomaterials. I. Microrheology of Type I Collagen Gels

Darrell Velegol* and Frederick Lanni†
*,†The Center for Light Microscope Imaging and Biotechnology, and †Department of Biological Sciences, Carnegie Mellon University, Pittsburgh, Pennsylvania 15213 USA

ABSTRACT A laser-trap microrheometry technique was used to determine the local shear moduli of Type I collagen gels. Embedded 2.1 μm polystyrene latex particles were displaced 10–100 nm using a near-infrared laser trap with a trap constant of 0.0001 N/m. The trap was oscillated transversely $\pm$200 nm using a refractive glass plate mounted on a galvanometric scanner. The displacement of the microspheres was in phase with the movement of the laser trap at frequencies less than 1 rad/s, indicating that at least locally, the gels behaved as elastic media. The local shear modulus was measured at various positions throughout the gel, and, for gels at 2.3 mg/mL and 37°C, values ranged from $G = 3$ to 80 Pa. The average shear modulus $G = 55$ Pa, which compares well with measurements from parallel plate rheometry.

INTRODUCTION

Collagen is a class of proteins found in human skin, bone, tendon, ligament, and connective tissue. It is a principle component of the extracellular matrix (ECM) in tissues (Hay, 1991; Alberts et al., 1994). Collagens constitute 25% of the total protein mass of multicellular animals (Alberts et al., 1994), and therefore they are a natural material to be used for tissue equivalents (Lanza et al., 1997). Of the collagen present in the body, about 90% is Type I. Type I collagen is soluble in dilute acid and can be obtained by extraction from rat tail tendon or bovine calf skin, among other sources (Elsdale and Bard, 1972a,b). Upon raising the pH and temperature to physiological conditions, a Type I collagen solution forms a hydrogel. Cells can be grown on this gel, which acts like an ECM. With time, the cells have two important mechanical effects on the hydrogel. 1) They cause the gel to shrink in volume by more than an order of magnitude. This occurs as the gel fibrils are compacted and water is lost through syneresis (Moon and Tranquillo, 1993; Barocas et al., 1995). 2) The collagen fibrils, which initially have a random orientation within the hydrogel, become aligned. This, in turn, causes a directed motility of cells along the fibrils (Dickinson et al., 1994). Both effects appear to be caused by the traction forces exerted by the cells on the hydrogel. The ultimate goal of our research project is to measure these traction forces and to understand their effect on the restructuring of the collagen gels.

The method we use to measure traction forces is based on Hooke's law from elasticity theory. When a linear spring is stretched by a displacement (Δx), the spring exerts a restoring force (F) given by $F = -k\Delta x$. If a load is applied to a spring with a known spring constant (k) and the resulting Δx is measured, Hooke's law gives the force. We use a similar concept, although the equations become tensorial (Dembo et al., 1996). By first measuring the mechanical properties of the gel and then measuring the deformation the cells cause in the gel, we use elasticity theory to calculate the traction forces that cells exert on collagen hydrogels. Dembo and Wang (1999) used this method to analyze traction forces on uniform, stiff polyacrylamide hydrogels. The Type I collagen hydrogels we work with are much less stiff, and include the possibility that the mechanical properties were nonuniform. We examined the gels using laser-trap microrheometry. The results of these measurements are reported in this paper.

Several researchers have studied the rheology of Type I collagen using macroscopic techniques. Hsu et al. (1994) used a cone-and-plate rheometer to study collagen hydrogels with a collagen concentration of 0.91 mg/mL. They examined how ionic strength and the presence of other macromolecular components (e.g., dermatan sulfate, hyaluronic acid, fibronectin, elastin) affected the rheology of the gels, finding elastic shear moduli from 10 to 100 Pa. Barocas et al. (1995) studied collagen at 2.1 mg/mL using Couette rheometry. The collagen gel behaved as a Maxwell fluid with a zero-shear viscosity of 7.4×10^5 Pa·s and a shear modulus of 15.5 Pa. Knapp et al. (1997) examined the rheology of collagen hydrogels in confined compression, which enabled them to examine the two-phase behavior of collagen gels (i.e., fibrils and water). Djabourov et al. (1993) and Newman et al. (1997) studied the rheology of collagen hydrogels during the gelation process. None of these studies examined local rheological properties, which we expected to be important on the 10–100-μm scale of single cells.

Various methods can be used to determine the microrheological characteristics of a sample. Manipulation of magnetic microparticles, coupled with video detection of nanometer displacements, was used by Guilford and Gore (1992) to study interstitial connective tissue. A similar method was used by Ziemann et al. (1994) to examine

Received for publication 21 July 2000 and in final form 24 May 2001.

Dr. Velegol's present address, and to whom reprint requests should be addressed, is Penn State University, Department of Chemical Engineering, 111 Fenske Lab, University Park, PA 16802. Tel.: 814-865-8739; Fax: 814-865-7846. E-mail: velegol@psu.edu.

0006-3495/01/09/1786/07 $2.00

entangled actin networks. Mason and Weitz (1995a,b) followed the Brownian motion of a particle with dynamic light scattering and interpreted the movements using a generalized Langevin equation. They were able to obtain G' and G'' for a suspension of silica particles in ethylene glycol (i.e., hard spheres) and a 15% solution of polyethylene oxide in water, showing good agreement with classical mechanical rheology measurements. Schnurr et al. (1997) developed a laser interferometry method that also used the Brownian motion of a particle to determine G' and G'' for semiflexible F-actin solutions and poly(acrylamide) gels. They consistently found that control measurements taken using a cone-and-plate rheometer were lower than the microrheometric measurements. Valentine et al. (1996) used a laser trap to manipulate a polystyrene latex particle immersed in a polymeric fluid (telechelic PEO). They observed bead movements using a position-sensitive detector. Although the authors measured only the viscous component of the fluid, they were the first to demonstrate the method of laser-trap microrheometry (see also Hough and Ou-Yang, 1999).

In this paper, we use the laser microrheometry technique to probe collagen gels on a micron-length scale. This method has the advantage that it can measure local mechanical properties in situ even as the cells exert traction on the gel, which is important because we expect the mechanical properties of the gel to change considerably over long time periods due to cell action. Not only do the properties of these gels change in magnitude with time, but significant heterogeneity of properties arises (Crocker et al., 2000), and, with time, the mechanical properties become anisotropic. This method is capable of measuring the rheology along two or three axes, although in this paper we measure the mechanical properties in one axis only.

MATERIALS AND METHODS

The Type I collagen hydrogel

Collagen gels were formed from Vitrogen 100 Type I collagen (No 98D241A , Collagen Corp.,). Vitrogen 100 is a purified, pepsin-solubilized bovine dermal collagen sold in solution at 3.0 mg/mL in 0.012 N HCl. It is 99.9% collagen, with 95–98% being Type I. Further information about Vitrogen 100 can be obtained from the Collagen Corporation. A hydrogel can be formed by neutralization of the collagen solution. Milliliter batches of collagen solutions at concentrations of 0.5–2.3 mg/mL were made by adding 0.1 N NaOH to the collagen solution, bringing the pH to 7.4. Sulfate-stabilized polystyrene latex microspheres (2.1 μm, Interfacial Dynamics Corporation, , Oregon) were added to the solution before gelation, along with phosphate buffer saline (PBS, pH 7.4) and enough water to give the final concentration. Solutions were injected into rectangular capillary tubes (Vitrocom, Mountain Lakes, NJ) of size ID = 0.20 mm, inner width = 2 mm, and length = 5 cm. The solutions were incubated in the capillary at 37°C for 60 min to cause gelation. The solutions showed no visible signs of gelation before the incubation process. Scanning electron micrographs (SEMs) of fixed gels in open containers show collagen fibrils in a felt-like, interconnected matrix (Fig. 1). The fibril matrix is also visible in hydrated gels when viewed by high-resolution differential interference contrast optical microscopy.

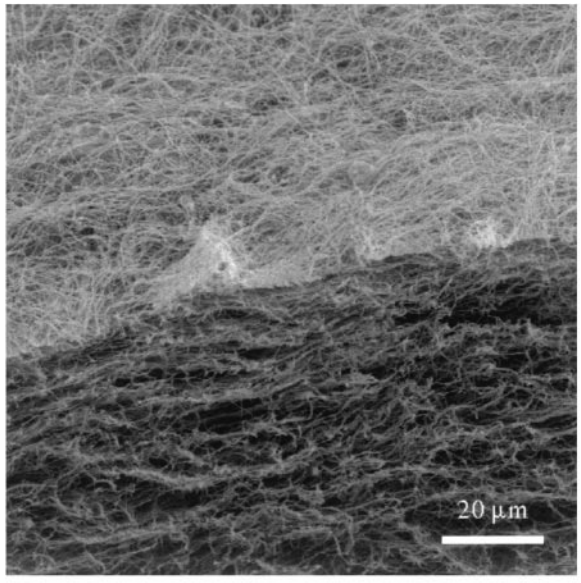

FIGURE 1 Scanning electron micrograph showing upper surface and cross-section of a 2.3-g/mL collagen gel. The gel was cut across with a razor blade after critical-point drying, but before metal shadowing.

Calibrating the laser trap

In our study, we used a variation of the laser-trap method given by Valentine et al. (1996), using digital video microscopy to obtain the position of individual particles to within ±2 nm (Gelles et al., 1988). A near-infrared diode laser (SDL-5762 MOPA laser, 1000 mW, 992 nm wavelength) was used to produce a laser trap (Svoboda and Block, 1994; Kuo, 1995) in an Axiovert 135TV microscope (Zeiss) equipped with a 100×, 1.25 NA oil-immersion objective. Transmitted-light images were captured with a C4880 CCD digital camera (Hamamatsu, Japan) operated via the custom software of our Automated Interactive Microscope (see Taylor et al., 1996). Eight-bit images (250×256 pixels) were acquired at 8–11 frames/sec. The power of the near-infrared laser could be controlled from 1 to 99% in 100 parts. The laser trap was oscillated ±200 nm using a refractive glass plate made of an ordinary microscope slide. The slide was mounted on a galvanometric scanner and oscillated rotationally (~±1°) at a rate of 0.06–60 rad/s (Fig. 2). The glass slide "beam steerer" shifted the laser beam by refraction, which caused movement of the beam focus in the transverse direction by roughly 100 μm. After demagnification through the microscope, the trap movement was measured to be ~190 nm. The precise number could be controlled by adjusting the amplitude of the galvanometer rotation. The custom software enabled us to know the precise time of image capture and the precise position of the beam steerer. The experimental setup of the laser trap is shown in Fig. 2.

Calibration of the laser trap was done using a standard hydrodynamic method with microspheres in a water specimen. The microscope stage was driven at various steady speeds from 0 to 100 μm/s (measured by watching the movement of nontrapped tracer particles), and the steady-state displacement of the trapped particle away from the center of the trap was measured using video microscopy (Gelles et al., 1988) and image processing.

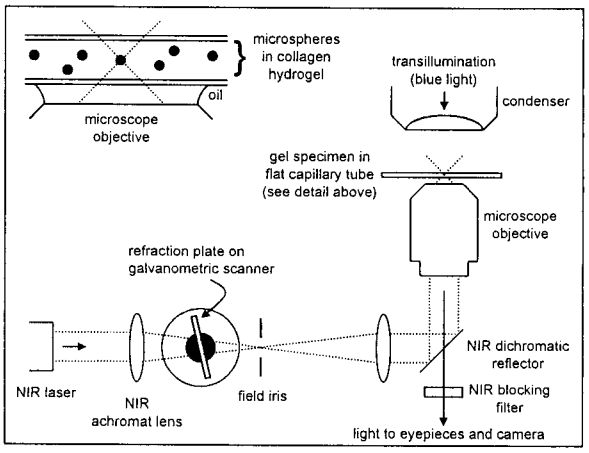

FIGURE 2 Schematic of the laser trap. The dotted lines represent the near-infrared laser radiation for the trap, whereas the solid lines indicate the transmitted light by which we are able to image the particle.

Particle position was defined by the center computed in NIH Image software as

$$\mathbf{x}_p = \frac{\iint_s \mathbf{x} f(\mathbf{x})\, dS}{\iint_s f(\mathbf{x})\, dS}, \quad (1)$$

where x_p represents the particle center; S represent the area over the whole object space; and $f(x)$ represents the local binary gray level, obtained by thresholding the image to black and white.

Two forces act on the particle during calibration: the optical force (F_L) holds the particle in the trap, and the hydrodynamic force (F_H) caused by the moving fluid displaces the particle from the trap center. For small displacements, F_L is given by

$$F_L = -k_L(x_p - x_L), \quad (2)$$

where k_L is the trap constant, x_p is the position of the particle center, and x_L is the position of the laser-trap center. We found this linear relation for $x_p - x_L < 200$ nm (Fig. 3). F_H is given approximately by Stokes law,

$$F_H = 6\pi\eta a U, \quad (3)$$

where η is the fluid viscosity, a is the particle radius, and U is the fluid velocity past the stationary particle. More sophisticated forms of Eq. 3 could have been used when the height (z) between the particle center and the capillary wall was small. However, for $z/a > 5$ (as in our experiments), Eq. 3 has less than 10% error (Goldman et al., 1967). Nevertheless, experimentally, we did calibrate the trap at various heights (z) above the capillary wall.

Because the particle was not accelerating, $F_L + F_H = 0$. Thus, Eqs. 2 and 3 give the trap constant k_L as a function of the fluid velocity (U) and displacement from the center of the trap. Figure 3 shows the linearity of the trap with displacement from the trap center (i.e., how well k_L remains constant). It is seen that, to within experimental uncertainty, the trap remains at roughly $k_L = 100$ μN/m for small ($x_p - x_L$) at full laser power. Figure 4 shows k_L for various heights (z) above the capillary surface. The dip near $z = 0$ is due to the error in Stokes law discussed above (i.e., we do not account for the glass surface). The decrease in k_L with z above 10

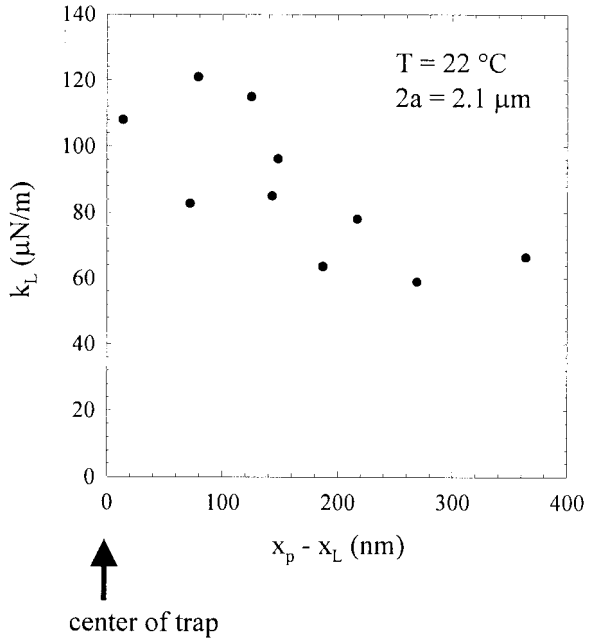

FIGURE 3 Calibration of the laser trap. The trap constant (k_L) is shown as a function of distance ($x_p - x_L$) of the particle from the center of the trap. The trap is linear to roughly 160 nm, but even at 200 nm, k_L is still 72% of the value near the center of the trap, which is 100 μN/m.

μm is due to optical aberration with depth of focus into the specimen. This originates in the refractive index mismatch between immersion oil (n = 1.52) and the gel (n = 1.33–1.34). Note that k_L = 0.00010 N/m at the maximum. Because our gels were less than 0.25% collagen, this trap constant should have remained unaffected by light scattering.

We calibrated the trap at various laser powers, and the trap constant remained proportional to the applied power. This indicates that the particle did not absorb a significant amount of laser energy. If this had occurred, the fluid around the particle would have increased in temperature, decreased in viscosity, and given a different laser-trap constant. In addition, in the collagen hydrogel, no change in gel fibrils (e.g., deformation or dissolution) was ever seen that indicated an elevated temperature field near the laser focus.

Laser trap microrheometry

After the trap was calibrated, collagen specimens containing identical particles were tested. Each test particle was centered into the trap using the motorized stage control and video microscopy. Alignment by eye was obtained to within 100 nm; one can align the center of objects much more accurately than the resolution limit of the microscope. Focus was set reproducibly by observing the central bright disk of the spheres. Misalignment at higher collagen concentrations (where the gel has a higher modulus) is more problematic than at low concentrations, because the laser trap then cannot pull the microsphere near to the center of the trap. On the contrary, at lower collagen concentrations, the hydrogel is sufficiently weak that the trap pulls the microsphere much closer to on-axis alignment.

After the alignment to a cross-hair was done, the laser trap and the beam steerer were turned on. Centration (and focus) error caused the test particle to "jump" when the trap was activated, and this was used as a cue to optimize further the centration. Thus, in hydrogels with a low collagen concentration (i.e., lower modulus), this jump allowed quicker centration of the microsphere.

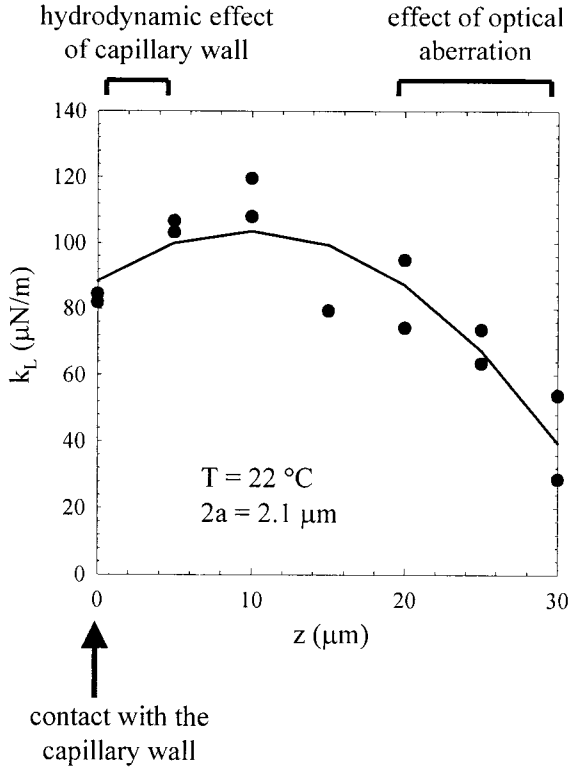

FIGURE 4 Effect of z position of microsphere on trap strength. The trap constant (k_L) is shown as a function of distance away from the lower wall of the chamber. At small z, the value of k_L appears to be reduced, because we neglect the hydrodynamic effect of the capillary wall. At large z the value of k_L is truly reduced due to optical aberration. In our experiments, z was kept at roughly 10 μm.

By assuming the collagen hydrogel acted as an elastic (E) material, the calculated force of the gel on a spherical particle is (Phan-Thien and Kim, 1994)

$$F_E = -24\pi G a \delta_x \left(\frac{1-\nu}{5-6\nu}\right), \quad (4)$$

where G is the storage modulus, a is the particle radius, and δ_x is the displacement of the sphere. For an incompressible material, $\nu = 0.5$. In this case, the term in parentheses is 0.25 and Stokes law for an elastic material is recovered. It is difficult to measure ν for a biphasic material like a collagen gel, but if we estimate the term in brackets to be 0.25, then the maximum error is about 10% from this equation because it is relatively insensitive to ν. We found no viscous behavior over short time periods (see Results), and, thus, Eq. 4 was used for all calculations. Other more sophisticated equations could have been used, including equations that account for viscoelasticity and anisotropy.

RESULTS

Figure 5 shows the results from a typical experiment in a collagen gel. With the trap off, the particle underwent small-amplitude, localized Brownian motion in the elastic medium (Mason and Weitz, 1995a; Schnurr et al., 1997). It was usually the case that the particle was not

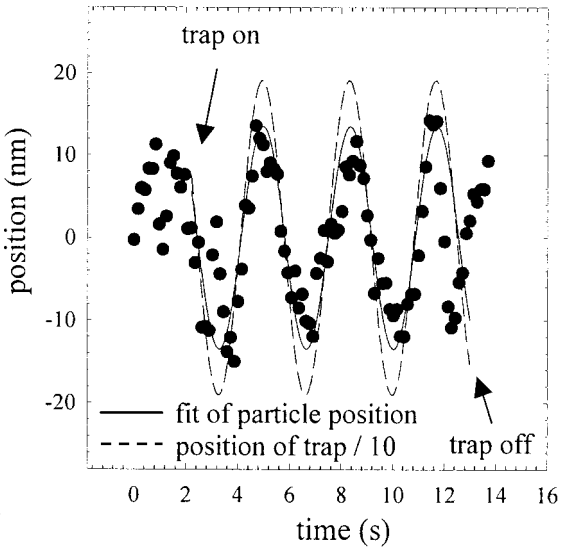

FIGURE 5 Position of trapped microsphere as a function of time. The 2.1-μm polystyrene latex particle was moved in a 2.3-mg/mL collagen gel at 22°C at a frequency of 2 rad/s. The displacement of the particle is given in nanometers. Note that, initially, before the trap is turned on, the microsphere is not centered with the trap. After the experiment (near 13 s), when the trap was released, the particle returned to its initial position.

initially centered on the trap (as shown in Fig. 5), as determined by comparison to the position of a trapped particle in water. Thus, when the trap was turned on, the particle jumped slightly. The positions in Fig. 5 were obtained by taking a moving average over three camera frames. Three frames takes roughly 0.38 s, which is much less than the time scale of ~3 s for particle movement. In all cases, the number of frames used in the moving average were much less than the time scale of movement (e.g., for the high frequencies, no moving average was possible). The moving average was used to reduce the effects of a drifting hydrogel (e.g., by up to 5 nm) during the experiment. The slow camera frame rate limited our temporal resolution, and, therefore, we were not able to detect viscous effects at high frequencies.

For all hydrogels tested, the shear modulus (G) was determined in the frequency range of 0.06–63 rad/sec at 22°C and 37°C (Fig. 6). The average G increases with collagen concentration as expected. However, the most striking pattern is the variation in shear moduli for the same concentration. Indeed, these same variations occurred within individual gels. For example, the 2.3-mg/mL gel has local shear moduli that vary from 2 to 90 Pa. This is not simply an experimental artifact. When viewing the specimen, most of the particles are visibly immobile (at least, to the resolution of the television system and human eye). However, some of the particles underwent visible Brownian motion. This Brownian motion gave no net displacement with time. Rather, it occurred within a harmonic well

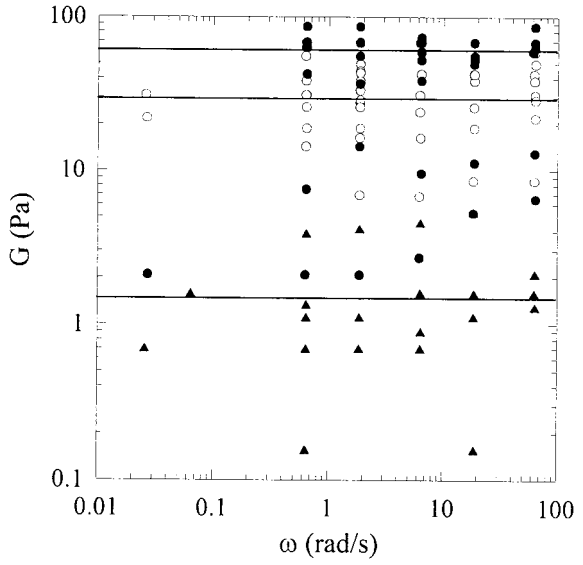

FIGURE 6 Shear modulus (G) for gels at 22°C. ●, 2.3 mg/mL; ○, 1.5 mg/mL; and ▲, 0.5 mg/mL. The lines give the average G at 2.3 mg/mL (*top line*), 1.5 mg/mL (*middle line*), and 0.5 mg/mL (*bottom line*). Note the large heterogeneity in properties with position for the same gel concentration.

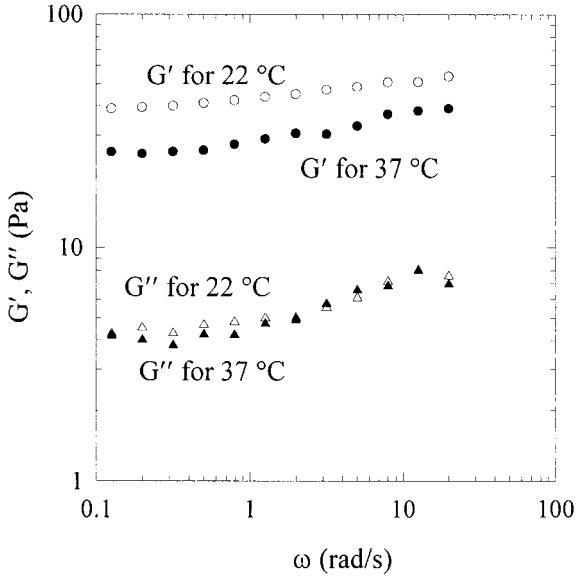

FIGURE 8 Rheological measurements from a macroscopic rheometer using a 40-mm parallel plate. The collagen concentration was 2.3 mg/mL, and the gap between the plates was 1 mm.

(Chandrasekar, 1943). This same behavior was seen in hydrogels at 37°C. Figures 6 and 7, which quantify both the trends and the heterogeneity in G, are the primary results of this paper.

The microscopic measurements give G values comparable to those obtained from our measurements using macroscopic rheometry (controlled stress Rheometrics Scientific SR-5). Neutralized, cold collagen solutions were brought to 37°C on the rheometer under zero shear conditions for 60 min until the hydrogels formed. For a few runs, we caused gelation under testing conditions; the gels appeared to be formed in ~10 min. After the gel was formed, the temperature was changed to the desired level over a period of 3 min. In our parallel-plate rheometer (40-mm plate, 1-mm gap), a large G' and a small G'' were relatively constant from 0.15 to 25 rad/s for both 22°C and 37°C (Fig. 8).

The linearity of the collagen gels was checked with a stress sweep. Barocas et al. (1995) showed that collagen is linear up to ~10% strain. Figure 9 shows that, for a collagen concentration of 0.5 mg/mL, the shear modulus of the hydrogel increased slightly with strain, but that, up to 10% strain, only a small variation in shear modulus (G) occurred. The nonlinearity probably occurs as the physical (i.e., noncovalent) bonds within the gel material break and reform, a process that increases at higher strains.

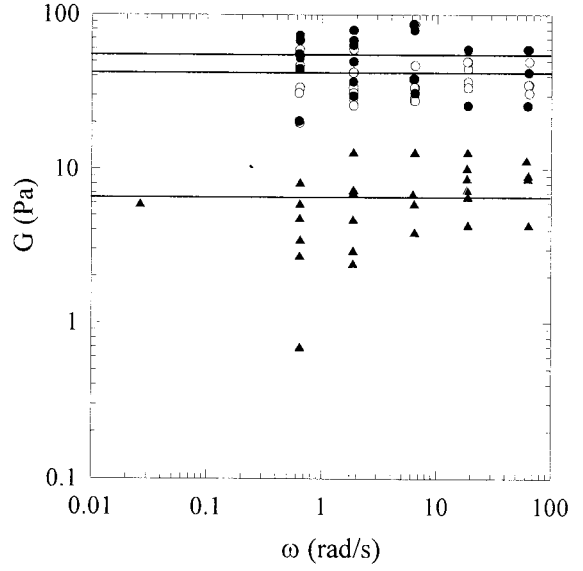

FIGURE 7 Shear modulus (G) for gels at 37°C. ●, 2.3 mg/mL; ○, 1.5 mg/mL; and ▲, 0.5 mg/mL. The lines give the average G at 2.3 mg/mL (*top line*), 1.5 mg/mL (*middle line*), and 0.5 mg/mL (*bottom line*).

DISCUSSION

The most striking feature of Figs. 6 and 7 is the significant variations in mechanical properties as a function of position within each gel matrix. Although we did not determine the precise length scale of this heterogeneity, we do know that, over length scales of 100 μm, the variations tend to average out. We determined this in experiments done with calibrated microneedles (data not shown), in which we applied a known force using the microneedle, and then obtained the material properties by observing the long-range deformation

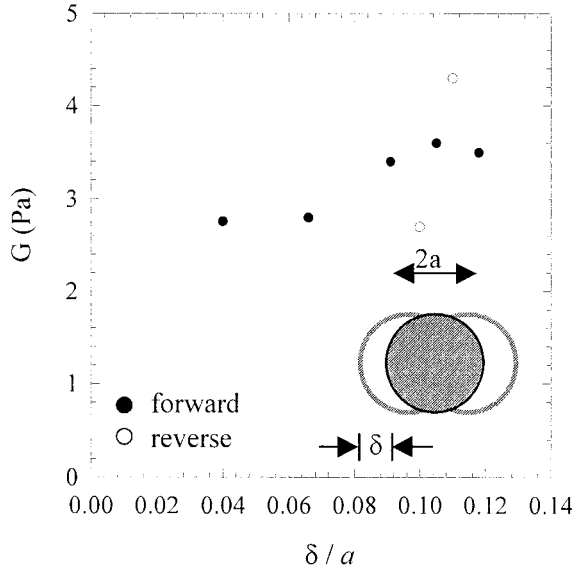

FIGURE 9 Linearity of collagen gel at 0.5 mg/mL. The gel is essentially linear Hookean up to 10% strain. *Forward* indicates an increasing strain amplitude, and *reverse* indicates decreasing strain amplitude.

field in the gel. The results indicate much smaller variation in mechanical properties. However, the focal adhesions between a fibroblast and its supportive collagen matrix are highly localized in the gel, and therefore the local characterization of the gel network is probably most relevant to cellular experiments. We did not determine whether the collagen concentration was altered in the immediate vicinity of the particle.

We do not detect the viscous portion of the modulus in microrheometry. This could be the result of our poor temporal resolution, because the imaging system attains Nyquist sampling for only the lower oscillation frequencies. With $f = 11$ frames/sec as our camera frame rate, our uncertainty in δ for $\tan\delta = G''/G'$ is ω/f (radians). So, to detect a $\tan\delta$ of 0.2 would require $\omega < 2.2$ rad/s for our camera frame rate. Thus, we would only detect the expected viscous behavior in our 0.6-rad/s measurements. Nevertheless, we do not detect viscous behavior even at this experimental frequency.

Overall, our results compare well with previous researchers, which are mentioned in the Introduction. Our parallel-plate measurements are comparable to, but slightly lower than, those obtained from laser-trap microrheometry. We cannot explain this difference, although it has been seen before (Schnurr et al., 1997). Although the proper method for averaging the mechanical properties for our hydrogel is unknown, the average shear modulus (G) from the microrheometry measurements does not depend strongly on the method of averaging. In the theory of mechanical properties for composites (Chawla, 1998; Christenson, 1979), there are two "rules of mixing" (Fig. 10): action in parallel (isostrain) and action in series (isostress). The equations of averaging for each are:

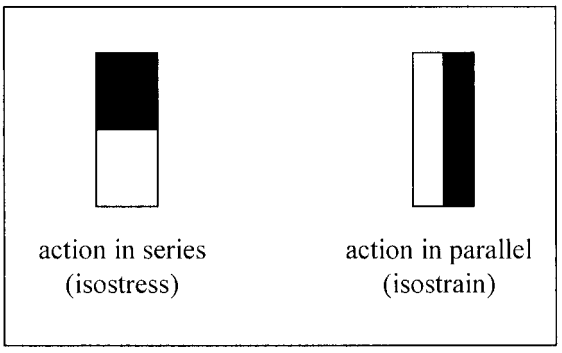

FIGURE 10 Rules of mixing for mechanical properties.

$$G_{\text{parallel}} = \sum \phi_i G_i, \tag{5}$$

$$G_{\text{series}} = \frac{1}{\sum \phi_i / G_i}. \tag{6}$$

In calculating averages, the ϕ_i were assumed to be $1/N$, where N is the number of measurements taken (i.e., each local value of G was weighted equally). For the 2.3-mg/mL gel at 37°C, the parallel rule gives $\langle G\rangle = 54$ Pa, whereas the series rule gives $\langle G\rangle = 45$ Pa. This occurs because the regions with low G (e.g., $G = 2$ Pa) have a higher impact on the average when used in the action-in-series model. Table 1 gives the average values for each gel concentration.

CONCLUSIONS

A laser-trap microrheometry technique was used to measure local mechanical properties in Type I collagen gels. The method can measure a frequency range of 0.06 to ~60 rad/s, and can measure heterogeneity and anisotropy in the mechanical properties. In the experiments reported here, it was shown that collagen gels (0.5–2.3 mg/mL) at 22°C and 37°C have shear moduli that vary from position to position. Although we have not yet determined the length scale of

TABLE 1 Gel properties from laser trap microrheometry averaged over local positions for $T = 37$°C

gel concentration (mg/mL)	$\langle G_{\text{isostress}}\rangle$ (Pa)	$\langle G_{\text{isostrain}}\rangle$ (Pa)
0.5	6.7 ± 0.57	4.55 ± 0.73
1.5	42 ± 2.4	38 ± 21
2.3	55 ± 3.9	47 ± 20

Each of the N local measurements of G in the various experiments were weighted equally (i.e., $\phi_i = 1/N$). The ± gives the standard error of the mean for the average value. The spread from position to position is shown clearly in Figs. 6 and 7. At each concentration, about thirty total samples were done. Note that, for the isostrain model, a few values far from the mean produce a large standard error.

this variation, the variation is large (e.g., for 2.3-mg/mL collagen gels, the local shear modulus varies from 2 to 90 Pa). Future experiments will be more involved, fully enabling the capability to measure anisotropic properties along multiple axes.

We thank G. Steven Vanni and Joseph Sukan for the scanning electron micrograph image in Fig. 1, Lynn Walker for her assistance and advice in doing the parallel-plate rheometry, and David Pane for his help in developing the Automated Interactive Microscope required to synchronize the galvanometric scanner and image acquisition. We also thank the National Science Foundation for funding through grant #MCB-8920118.

REFERENCES

Alberts, B., D. Bray, J. Lewis, M. Raff, K. Roberts, and J. D. Watson. 1994. Molecular Biology of the Cell, 3rd ed. Garland Publishing, New York.

Barocas, V. H., A. G. Moon, and R. T. Tranquillo. 1995. The fibroblast-populated collagen microsphere assay of cell traction force—Part 2: measurement of the cell traction parameter. *J. Biomech. Engr.* 117: 161–170.

Barocas, V. H., and R. T. Tranquillo. 1997. An anisotropic biphasic theory of tissue-equivalent mechanics: the interplay among cell traction, fibril network deformation, and contact guidance. *J. Biomech. Engr.* 119: 137–145.

Bell, E., B. Ivarsson, and C. Merrill. 1979. Production of a tissue-like structure by contraction of collagen lattices by human fibroblasts of different proliferative potential in vitro. *Proc. Natl. Acad. Sci. U.S.A.* 76:1274–1278.

Chandrasekhar, S. 1943. Stochastic problems in physics and astronomy. *Rev. Mod. Phys*. 15:1–74. This article appears in the book edited by N. Wax. 1954. Selected Papers on Noise and Stochastic Processes. Dover, New York.

Chawla, K. K. 1998. Composite Materials: Science and Engineering. Springer, New York.

Christenson, R. M. 1979. Mechanics of Composite Materials. Wiley, New York.

Crocker, J. C., M. T. Valentine, E. R. Weeks, T. Gisler, P. D. Kaplan, A. G. Yodh, D. A. Weitz. 2000. Two-point microrheology of inhomogeneous soft materials. *Phys. Rev. Lett.* 85:888–891.

Dembo, M., T. Oliver, A. Ishihara, and K. Jacobson. 1996. Imaging the traction stresses exerted by locomoting cells with the elastic substratum method. *Biophys. J.* 70:2008–2022.

Dembo, M., and Y. Wang. 1999. Stresses at the cell-to-substrate interface during locomotion of fibroblasts. *Biophys. J.* 76:2307–2316.

Dickinson, R. B., S. Guido, and R. T. Tranquillo. 1994. Biased cell migration of fibroblasts exhibiting contact guidance in oriented collagen gels. *Ann. Biomed. Eng.* 22:342–356.

Djabourov, M., J. Lechaire, and F. Gaill. 1993. Structure and rheology of gelatin and collagen gels. *Biorheology.* 30:191–205.

Elsdale, T., and J. Bard. 1972a. Collagen substrata for studies on cell behavior. *J. Cell Biol.* 52:626–637.

Elsdale, T., and J. Bard. 1972b. Cellular interactions in mass cultures of human diploid fibroblasts. *Nature.* 236:152–155.

Gelles, J., B. J. Schnapp, and M. P. Sheetz. 1988. Tracking kinesin-driven movements with nanometre-scale precision. *Nature.* 331:450–453.

Goldman, A. J., R. G. Cox, and H. Brenner. 1967. Slow viscous motion of a sphere parallel to a plane wall—I. Motion through a quiescent fluid. *Chem. Eng. Sci.* 22:637–651.

Guilford, W. H., and R. W. Gore. 1992. A novel remote-sensing isometric force transducer for micromechanics studies. *Am. J. Physiol. Cell Physiol*. 32:C700–C707.

Hay, Elizabeth D. 1991. Cell Biology of Extracellular Matrix, 2nd ed. Plenum Press, New York.

Hough, L. A., and H. D. Ou-Yang. 1999. A new probe for mechanical testing of nanostructures in soft materials. *J. Nanoparticle Res*. 1:495–499.

Hsu, S., A. M. Jamieson, and J. Blackwell. 1994. Viscoelastic studies of extracellular matrix interactions in a model native collagen gel system. *Biorheology.* 31:21–36.

Knapp, D. M., V. H. Barocas, A. G. Moon, K. Yoo, L. R. Petzold, and R. T. Tranquillo. 1997. Rheology of reconstituted Type I collagen gel in confined compression. *J. Rheol.* 41:971–993.

Kuo, S. C. 1995. Optical tweezers: a practical guide. *J. Microscopy Soc. Amer.* 1:65–74.

Kuo, S. C., J. Gelles, E. Steuer, and M. P. Sheetz. 1991. A model for kinesin movement from nanometer-level movements of kinesin and cytoplasmic dynein and force measurements. *J. Cell Sci.* 14:135–138.

Lanza, R. P., R. Langer, and W. L. Chick. 1997. Principles of Tissue Engineering. Academic Press, San Diego, CA.

Mason, T. G., and D. A. Weitz. 1995a. Optical measurements of frequency-dependent linear viscoelastic moduli of complex fluids. *Phys. Rev. Let.* 74:1250–1253.

Mason, T. G., and D. A. Weitz. 1995b. Linear viscoelasticity of colloidal hard sphere suspensions near the glass transition. *Phys. Rev. Let.* 75: 2770–2773.

Moon, A. G., and R. T. Tranquillo. 1993. The fibroblast-populated collagen microsphere assay of cell traction force—Part 1: continuum model. *AIChE J.* 39:163–177.

Newman, S., M. Cloitre, C. Allain, G. Forgacs, and D. Beysens. 1997. Viscosity and elasticity during collagen assembly in vitro: relevance to matrix-driven translocation. *Biopolymers.* 41:337–347.

Phan-Thien, N., and S. Kim. 1994. Microstructures in Elastic Media. Oxford University Press, New York.

Schnurr, B., F. Gittes, F. C. MacKintosh, and C. F. Schmidt. 1997. Determining microscopic viscoelasticity in flexible and semiflexible polymer networks from thermal fluctuations. *Macromolecules.* 30: 7781–7792.

Svoboda, K., and S. M. Block. 1994. Biological applications of optical forces. *Annu. Rev. Biophys. Biomol. Struct.* 23:247–285.

Taylor, D. L., L. D. Harris, R. DeBiasio, S. E. Fahlman, D. L. Farkas, F. Lanni, M. Nederlof, A. H. Gough. *Proc. Soc. Photo-Optical Instr. Eng.* 2678:15–27.

Valentine, M. T., L. E. Dewalt, and H. D. Ou-Yang. 1996. Forces on a colloidal particle in a polymer solution: a study using optical tweezers. *J. Phys. Condens. Matter.* 8:9477–9482.

Ziemann, F., J. Radler, and E. Sackmann. 1994. Local measurements of viscoelastic moduli of entangled actin networks using an oscillating magnetic bead micro-rheometer. *Biophys. J.* 66:2210–2216.